https://doi.org/10.20965/jrm.1995.p0467

Paper:

Motion Control of a Piezopolymer Bimorph Flexible Microactuator

Minoru Sasaki and Masayuki Okugawa

Department of Mechanical Engineering, Faculty of Engineering, Gifu University
1-1 Yanagido, Gifu, 501-11 Japan
[Received October 25, 1995; accepted November 10, 1995]

An optimal feedback control of a flexible microactuator made of a bimorph piezoelectric high-polymer material (PVDF: Poly Vinylidene Fluoride), is proposed in this paper. This optimal feedback control is based on the assumption that the full state vector of the system is available for measurement although practically all state variables are very difficult to measure in the case of a distributed parameter system. An observer is used to estimate the entire state vector of the system, but the presence of sensor noise tends to adversely affect the convergence of the observer. This naturally leads to a stochastic observer commonly known as the Kalman filter. Numerical and experimental results demonstrate the effectiveness of the proposed controller design method.

Keywords: Motion control of an actuator, Kalman filter, Optimal tracking system, Piezoelectric-polymer actuator, **PVDF**

I. Introduction

In simple terms, Micro-robots are automatically controlled fine motion positioners. Although their features may be substantially bigger than a micron, the motion resolution sought is on the micron level or smaller. Many operations in semiconductor manufacturing such as probing and wire bonding require high-precision controlled motion and delicate forces. Such operations have resisted automation because of the inherent friction which limits the repeatability and resolution of robots and other automated tools. Also, in biomedical research, biosubstance processing, and micro-gravity material processing, it is of interest to select and manipulate objects which are microscopic in size, ranging from a few millimeters to several microns in diameter. The manipulation of these microscopic objects calls for the development of special end-effectors which differ greatly from those in conventional actuators.

In this paper, we make use of the piezoelectric effect in polymers to develop microactuators. Although more than one hundred years ago, the Curie brothers discovered that quartz crystals produce an electrical charge when deformed,[1] they also found that the same crystals change in dimension when subjected to an electric field. One of the practical applications of this technology was made by Langevin.[2] He built a quartz transmitter and receiver for underwater sound that became the first sonar. In the following decades, piezoelectric activity was found in a number of natural and synthetic single-crystal materials and the effect was widely utilized. By the 1960s, attention was first given to piezoelectric effects in organic materials. In 1969, Kawai discovered the strong piezoelectric effect in **PVDF** or **PVF$_2$** (poly vinylidene fluoride).[3] Compared to other piezoelectric materials, **PVDF** has certain unique properties such as high levels of piezo activity, an extremely wide frequency range, a broad dynamic response, and low acoustic impedance.[4-7] This makes it attractive for many sensor and transducer applications. In simple terms, a bimorph is composed of two pieces of metallized **PVDF** layers glued together to form a laminate. When a voltage is applied across the elements, one element elongates and, the other shorten producing a deflection. **PVDF** bimorphs provide answers to many of the problems associated with implementing light-weight compact, and simple electromotional devices. To model the piezopolymer microactuator under applied electric fields, we applied the classical laminate beam theory. We assumed that the laminate is perfectly bonded, and that Kirchhoff's conditions are satisfied.

An optimal feedback control of a flexible microactuator made of a bimorph piezoelectric high-polymer material is proposed in this paper. This optimal feedback control is based on the assumption that the full state vector of the system is available for measurement, although practically all state variables are very difficult to measure in the case of a distributed parameter system. An observer is used to estimate the entire state vector of the system. For fast convergence, the observer poles should be deep in the left half of the complex plane, which implies a large gain matrix. However, a large gain matrix makes the observer sensitive to sensor noise which is superimposed to the original system output vector. Noise is stochastic in nature, and its characteristics are generally described in terms of statistical quantities. The presence of sensor noise tends to adversely affect the convergence of an observer. This naturally leads to a stochastic observer known as the Kalman filter that not only can handle noise better but also is characterized by observer gains that are optimal in some sense.

The step response of the system indicates that the output quickly tracks reference input without overshooting. Numerical and experimental results illustrate the effectiveness of the proposed controller design method of a flexible microactuator.

2. Modeling of the Flexible Microactuator

Figure 1 shows the piezopolymer bimorph flexible microactuator model. The piezopolymer bimorph microactuator consists of two **PVDF** films cemented with a metal shim in proper polarity. When an electric voltage is applied to the terminals of the actuator, one film expands while the other contracts. As a result, the actuator bends as shown in **Fig.2**. Expanding Kirchhoff's hypothesis, which results in a plane stress state for a thin beam, to piezoelectric lamina will yield the following constitutive equations of each lamina.

$$\varepsilon_1 = \frac{T_1}{E_1} + d_1 v_1 \quad \dots\dots\dots\dots (1)$$

$$\varepsilon_2 = \frac{T_2}{E_2} \quad \dots\dots\dots\dots (2)$$

$$\varepsilon_3 = \frac{T_3}{E_3} + d_3 v_3 \quad \dots\dots\dots\dots (3)$$

where the ε_i, T_i, E_i, d_i, v_i represent the strain, stress, Young's modulus, piezoelectric strain/charge constants, and electric field, respectively. The subscript i implies the ith lamina of the laminate. The bending moment about the y-axis is

$$M(x) = b\int_{Y_0 - c_2 - c_3}^{Y_0 + c_1 + c_2} Tydy \quad \dots\dots (4)$$

where b is the width of the actuator, and y is the distance in the y-axis direction from the neutral surface of the actuator. The relationships between the strains and bending displacement are given by

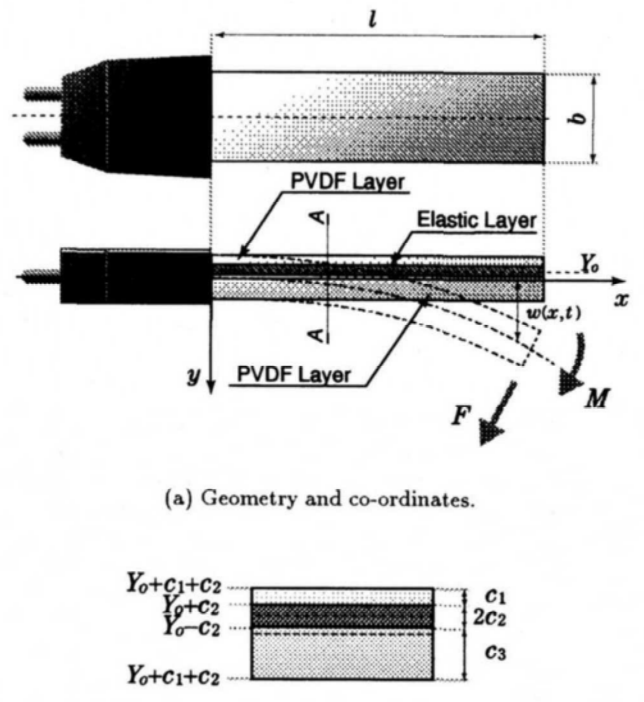

(a) Geometry and co-ordinates.

(b) Detailed cross section A-A.

Fig. 1. Microactuator model.

$$\varepsilon_{1,2,3} = y\frac{\partial^2 w(x,t)}{\partial x^2} \quad \dots\dots\dots\dots (5)$$

Substituting Eq.(5) into Eqs.(1)-(3) yields:

$$T_1 = yE_1\frac{\partial^2 w(x,t)}{\partial x^2} - d_1 E_1 v_1 \quad \dots\dots\dots\dots (6)$$

$$T_2 = yE_2\frac{\partial^2 w(x,t)}{\partial x^2} \quad \dots\dots\dots\dots (7)$$

$$T_3 = yE_3\frac{\partial^2 w(x,t)}{\partial x^2} - d_3 E_3 v_3 \quad \dots\dots\dots\dots (8)$$

Eq.(4) is integrated through the thickness of the laminate, and the following equations are obtained:

$$M(x) = b\int_{Y_0 - c_2 - c_3}^{Y_0 + c_1 + c_2} E\frac{\partial^2 w(x,t)}{\partial x^2} y^2 dy - b\int_{Y_0 - c_2 - c_3}^{Y_0 + c_1 + c_2} dEvydy \quad \dots (9)$$

$$= -(E_1 I_1 + E_2 I_2 + E_3 I_3)\frac{\partial^2 w(x,t)}{\partial x^2} + \left(\frac{d_1 E_1 z_1}{c_1} - \frac{d_3 E_3 z_3}{c_3}\right)V(t) \quad \dots (10)$$

where

$$Y_0 = \frac{E_3(c_3^2 + 2c_3c_2) - E_1(c_1^2 + 2c_1c_2)}{(E_1c_1 + 2E_2c_2 + E_3c_3)} \quad \dots (11)$$

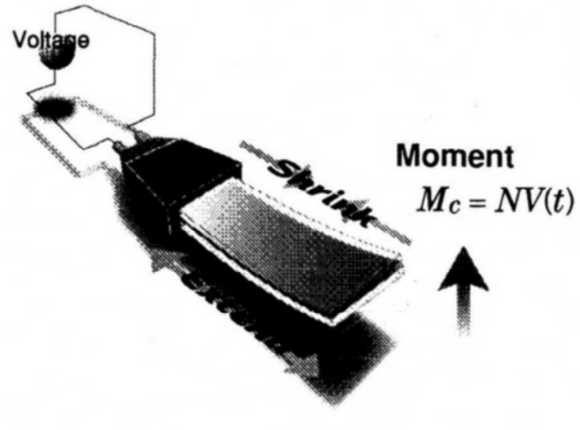

Fig. 2. Actuator motion.

$$z_1 = b \int_{Y_0+c_2}^{Y_0+c_1+c_2} y dy = bc_1 \left(Y_0 + \frac{c_1}{2} + c_2\right) \quad (12)$$

$$z_3 = b \int_{Y_0-c_2-c_3}^{Y_0+c_2} y dy = bc_3 \left(Y_0 + \frac{c_3}{2} + c_2\right) \quad (13)$$

$$I_1 = b \int_{Y_0+c_2}^{Y_0+c_1+c_2} y^2 dy = bc_1 \left\{Y_0^2 + (c_1 + 2c_2)Y_0 + \frac{c_1^2}{3} + c_1c_2 + c_2^2\right\} \quad (14)$$

$$I_2 = b \int_{Y_0-c_2}^{Y_0+c_2} y^2 dy = 2bc_2 \left(Y_0^2 + \frac{c_2^2}{3}\right) \quad (15)$$

$$I_3 = b \int_{Y_0-c_2-c_3}^{Y_0+c_2} y^2 dy = bc_3 \left\{Y_0^2 - (c_3 + 2c_2)Y_0 + \frac{c_3^2}{3} + c_3c_2 + c_2^2\right\} \quad (16)$$

Now considering the end point force F, moment M, and structural damping, the equation of motion of the actuator is given by

$$\frac{\partial^2}{\partial x^2}\left\{EI\left(1 + \gamma\frac{\partial}{\partial t}\right)\frac{\partial^2 w(x,t)}{\partial x^2} - NV(t)\right\} + \rho A \frac{\partial^2 w(x,t)}{\partial t^2} = 0 \quad (17)$$

where ρ is the equivalent density of the laminate and γ is the structural damping coefficient and

$$E_1I_1 + E_2I_2 + E_3I_3 = EI \quad (18)$$

$$\frac{d_1E_1z_1}{c_1} - \frac{d_3E_3z_3}{c_3} = N \quad (19)$$

$$b(\rho_1c_1 + 2\rho_2c_2 + \rho_3c_3) = \rho A \quad (20)$$

The boundary conditions are

$$w(0,t) = 0 \quad (21)$$

$$\frac{\partial w(x,t)}{\partial x} = 0 \quad (22)$$

$$EI\left(1 + \gamma\frac{\partial}{\partial t}\right)\frac{\partial^2 w(l,t)}{\partial x^2} - NV(t) - M = 0 \quad (23)$$

$$EI\left(1 + \gamma\frac{\partial}{\partial t}\right)\frac{\partial^3 w(l,t)}{\partial x^3} + F = 0 \quad (24)$$

The solution of Eq.(17) is assumed to be of the form

$$y(x,t) = X(x)f(t) = \sum_{i=1}^{\infty} X_i(x)f_i(t) \quad (25)$$

where $X_i(x)$ is the ith mode function satisfying the boundary conditions given by Eqs. (21)-(24), and $f_i(t)$ is the corresponding time function.

For simplicity's sake, we let F and M be equal to zero. Substituting Eq.(25) into Eq.(17) and then applying the Galerkin method and adopting orthogonality of the normal function, yields a set of uncoupled model equations:

$$\ddot{f}_i(t) + \gamma\omega_i^2 X_i(l)\dot{f}_i(t) + \omega_i^2 f_i = \frac{N}{\rho A}\frac{dX_i(l)}{dx}V(t) \quad (26)$$

The ith order mode state vector is

$$\boldsymbol{x}_i = [f_i(t)\ \ \dot{f}_i(t)]^T$$

This model is an infinite degree of freedom system. It is generally difficult to design a control system for such a model, and it is impossible to make such a complete mathematical model of it.

Figure 3 illustrates the power spectrum of the response of the actuator after subjecting its input to a random signal. From this figure it can be seen that the 1st and 2nd mode are well pronounced. Consequently, the Eq.(26) is rewritten in the form of a state equation by truncating the model to the 2nd mode.[12] The state equation is

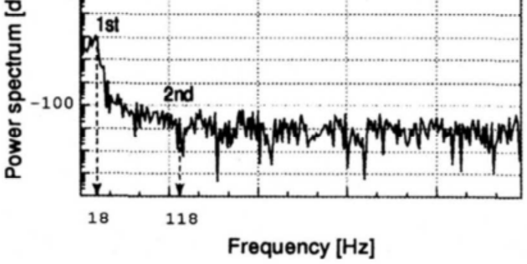

Fig. 3. Power spectrum of the object system under random input. (Experimental results)

$$\dot{\boldsymbol{x}}(t) = \boldsymbol{A}\boldsymbol{x}(t) + \boldsymbol{b}V(t) \quad \text{(27a)}$$

and the output equation is given by

$$y(t) = \boldsymbol{c}\boldsymbol{x}(t) \quad \text{(27b)}$$

where y is the bending displacement,

$$\boldsymbol{A} = \begin{bmatrix} \boldsymbol{A}_1 & \boldsymbol{0} \\ \boldsymbol{0} & \boldsymbol{A}_2 \end{bmatrix}, \quad \boldsymbol{b} = \begin{bmatrix} \boldsymbol{b}_1 \\ \boldsymbol{b}_2 \end{bmatrix}, \quad \boldsymbol{c} = [c_1 \;\; c_2]$$

Each of the ith order mode elements is

$$\boldsymbol{A}_i = \begin{bmatrix} 0 & 1 \\ -\omega_i^2 & -\gamma\,\omega_i^2 \end{bmatrix}, \quad \boldsymbol{b}_i = \begin{bmatrix} 0 \\ \dfrac{N}{\rho A}\dfrac{dX_i(l)}{dx} \end{bmatrix},$$

$$\boldsymbol{c}_i = [X_i(l) \;\; 0]$$

3. Optimal Estimation Using the Kalman Filter

Having designed the control law assuming that the entire state vector is available, implementing it using the entire estimated states makes the design of an optimal regulator complete. However, the entire state vector is practically very difficult to measure in the case of the distributed-parameter system. An observer can estimate the entire state vector when provided with measurements of the system parameters indicated by the output. The presence of sensor noise tends to affect the convergence adversely which leads naturally to a stochastic observer.[14] In the presence of noise, the object system (27a) (27b) can be rewritten as a *linear time invariant stochastic system governed by*

$$\dot{\boldsymbol{x}}(t) = \boldsymbol{A}\boldsymbol{x}(t) + \boldsymbol{b}V(t) + \boldsymbol{w}(t) \quad \text{(28a)}$$

$$y(t) = \boldsymbol{c}\boldsymbol{x}(t) + \sigma(t) \quad \text{(28b)}$$

where the system noise $\boldsymbol{w}(t)$ and the output noise $\sigma(t)$ are random sequences with zero mean and have covariances defined by Eq. (29).

$$E[\boldsymbol{w}(t)] = E[\sigma(t)] = 0$$

$$E\left\{\begin{bmatrix} \boldsymbol{w}(t) \\ \sigma(t) \end{bmatrix} [\boldsymbol{w}^T(\tau) \;\; \sigma^T(\tau)]\right\} = \begin{bmatrix} \boldsymbol{G} & 0 \\ 0 & \boldsymbol{Q} \end{bmatrix} \delta(t-\tau) \quad \text{(29)}$$

where $E[*]$ indicates expectation, $\boldsymbol{G}$ is a positive semi-definite matrix, $\boldsymbol{Q}$ is a positive definite matrix, and $\delta(x)$ is Dirac's delta function.

The Kalman filter is given by

$$\dot{\hat{\boldsymbol{x}}}(t) = \boldsymbol{A}\hat{\boldsymbol{x}}(t) + \boldsymbol{b}V(t) + \boldsymbol{H}(y(t) - \boldsymbol{c}\hat{\boldsymbol{x}}(t)) \quad \text{(30)}$$

$$= (\boldsymbol{A} - \boldsymbol{H}\boldsymbol{c})\hat{\boldsymbol{x}}(t) + \boldsymbol{b}V(t) + \boldsymbol{H}y(t) \quad \text{(31)}$$

where $\boldsymbol{H}$ is a feedback gain which gives vector $\hat{\boldsymbol{x}}(t)$ that estimates the state vector $\boldsymbol{x}(t)$ using the system input and output data. The estimation error $\varepsilon(t)$ is

$$\varepsilon(t) = \boldsymbol{x}(t) - \hat{\boldsymbol{x}}(t) \quad \text{(32)}$$

Subtracting Eq. (31) from Eq. (28a), we obtain

$$\dot{\varepsilon}(t) = (\boldsymbol{A} - \boldsymbol{H}\boldsymbol{c})\,\varepsilon(t) + \boldsymbol{w}(t) - \boldsymbol{H}\sigma(t) \quad \text{(33)}$$

The design of the Kalman filter is optimal because it selects the value of $\boldsymbol{H}$ which minimizes the cost function

$$J_0 = E[\varepsilon^T(t)\,\varepsilon(t)] \quad \text{(34)}$$

The optimal value of $\boldsymbol{H}$ is defined by

$$\boldsymbol{H} = \boldsymbol{P}_0\,\boldsymbol{c}^T\boldsymbol{Q}^{-1} \quad \text{(35)}$$

where $\boldsymbol{P}_o$ is the variance matrix of $\varepsilon(t)$ satisfying the Riccati equation.

$$\boldsymbol{A}\boldsymbol{P}_0 + \boldsymbol{P}_0\boldsymbol{A}^T - \boldsymbol{P}_0\boldsymbol{c}^T\boldsymbol{G}^{-1}\boldsymbol{c}\boldsymbol{P}_0 + \boldsymbol{Q} = \boldsymbol{0} \quad \text{(36)}$$

4. Tracking Controller Design for the Actuator

We now present an analytical approach to give a control system the ability to track (with zero error) a nondecaying input and to reject (with zero error) a nondecaying disturbance such as a step function. The method is based on the inclusion of the equations satisfied by these external signals as part of the problem formulation and solving the problem of control in an error space so that we are assured that the error approaches zero even if the output is following a step command.

Suppose we have the state Eqs.(27a) and (27b) and we wish to accomplish an optimal regulator design; and at the same time, we design a controller so that the closed-loop system can track an input with zero steady-state error and reject disturbances without error. Consider the case of tracking a constant input. In terms of u and $\boldsymbol{x}$ we have the control law.

$$\begin{aligned} \dot{u} &= -\boldsymbol{K}_1\dot{\boldsymbol{x}} + \boldsymbol{K}_2\dot{z} \\ &= -[\boldsymbol{K}_1 \;\; \boldsymbol{K}_2]\begin{bmatrix} \boldsymbol{A} & \boldsymbol{b} \\ \boldsymbol{c} & 0 \end{bmatrix}\begin{bmatrix} \boldsymbol{x} \\ u \end{bmatrix} + \boldsymbol{K}_2 u_r \end{aligned} \quad \text{(37)}$$

We only need to integrate (37) in order to reveal the control law and the action of integral control.

$$u = K_2 \int_0^t e d\tau - K_1 x \qquad (38)$$
$$= -K_1 x + K_2 z$$

$$\dot{z} = -c x + u_\tau \qquad (39)$$

A block diagram of the system is provided in **Fig.4**; it clearly indicates the presence of a pure integrator in the controller. This is a case of the internal-model principle, which requires a model of exogenous signal in the controller for robust tracking and disturbance rejection.[15]

One way to formulate the tracking problem is by differentiating the error equation and introducing the error as a state. To obtain the overall state vector the plant state vector is replaced by the state in error space defined by

$$\delta x(t) = \begin{bmatrix} x(t) - x(\infty) \\ u(t) - u(\infty) \end{bmatrix}$$

Let us consider the steady state error $e(t)$ defined by

$$e(t) = y(t) - u_\tau(t) \qquad (40)$$

where $u_r(t)$ is the reference input, $y(t)$ is the sensor output.

The error system for $\delta x(t)$ is then given by

$$\left.\begin{aligned} \delta\dot{x}(t) &= A^{\#}\delta x(t) + b^{\#} v(t) \\ e(t) &= c^{\#}\delta x(t) \end{aligned}\right\} \qquad (41)$$

where

$$v(t) = -F_e \delta x(t), \quad F_e = [K_1 \ \ K_2]\, E$$

$$A^{\#} = \begin{bmatrix} A & b \\ 0 & 0 \end{bmatrix}, \quad b^{\#} = \begin{bmatrix} 0 \\ 1 \end{bmatrix},$$
$$c^{\#} = [c \ \ 0], \quad E = \begin{bmatrix} A & b \\ c & 0 \end{bmatrix} \qquad (42)$$

The commonly chosen performance functional is

$$J = \int_0^\infty (e^T W e + v^T R v)\, dt \qquad (43)$$

*where v is the optimal control input, W is a positive semi-*definite error weighing matrix and R is a positive definite control weighing matrix.

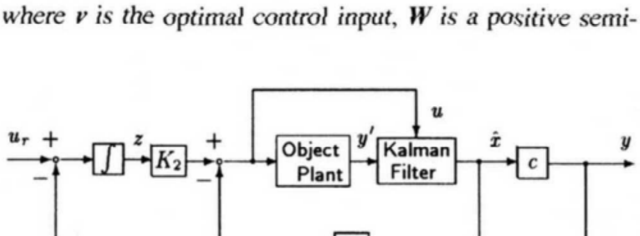

Fig. 4. Block diagram of LQG controller.

The optimal control input $v(t)$ which minimizes the performance function J is given by

$$v(t) = -R^{-1} b^{\#T} P \delta x(t) \qquad (44)$$

where P is the positive semi-definite solution of the Ricaati equation.

$$A^{\#T}P + PA^{\#} + Q - PbR^{-1}b^{\#T}P = 0 \qquad (45)$$

Consequently, the feedback gains $[K_1 \ K_2]$ are determined from Eq. (42) and Eq. (44).

$$[K_1 \ \ K_2] = R^{-1} b^{\#T} P E^{-1} \qquad (46)$$

Finally, the total system is expressed as

$$\begin{bmatrix} \dot{\hat{x}} \\ \dot{u} \end{bmatrix} = \begin{bmatrix} A & B \\ -K_1 A - K_2 c & -K_1 b \end{bmatrix} \begin{bmatrix} \hat{x} \\ u \end{bmatrix} + \begin{bmatrix} 0 \\ K_2 \end{bmatrix} u_r$$

$$y = [c \ \ 0] \begin{bmatrix} \hat{x} \\ u \end{bmatrix} \qquad (47)$$

5. Results and Discussion

Recently, stimulated by micro-processor technology, there is an increasing interest in issues related to digital control implementation. For the implementation of the designed LQG controller, we routinely use the TMS320C31-based digital signal processing system DSP-CIT, along with a set of design and implementation software tools, including an automatic code generator. The DSP-CIT combines the TMS320C31's tremendous computing performance of up to 40[MFlops] with a versatile set of on-board I/O: four analog input channels (16bit, 10[μsec] and 12bit 3[μsec]), four analog output channels (12bit), two incremental encoder channels and a complete subsystem for digital I/O.

We performed the design in the analogue domain using *MATLAB*,[16] and discretized the controller, after checking for the discretization, computational delays, and A/D- and D/A-quantization, the signal processor code was generated and downloaded. The sampling period was about 1[msec]. A reference signal is a square wave of 5.00[μm] height and a 4 second period. **Figure 5** presents the experimental setup of the discrete optimal servo system.

Figure 6(a) shows the experimental step response of the system without a controller. This result has a large overshoot and residual vibrations. It is apparent from the figure that the first natural frequency is predominant over other modal frequencies. The output signal contains white noise and the covariance is 6.20×10^{-8}. Figure 6(c) illustrates the numerical step response of the system without a controller. **Figure 7**(a) shows the experimental step response of the

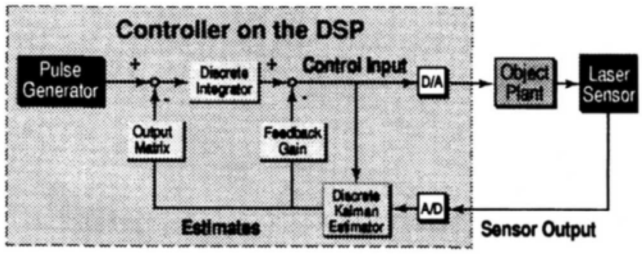

Fig. 5. Discrete optimal servo system.

system using the LQG controller with the weighing matrix $W = 1.0$ and $R = 5.0 \times 10.^{-4}$ Figure 7(b) presents the power spectrum of the system. Figure 7(c) illustrates the numerical step response of the system using the LQG controller. It is found that the result has a flat spectrum over the visible range. It is apparent that the experimental and numerical results are in good agreement with each other. The response in Fig.7(a) and (c) are identical to those of the input signals and in fact, almost indistinguishable from them.

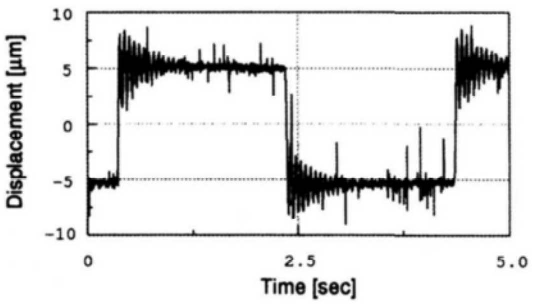

(a) Step response - Experimental results.

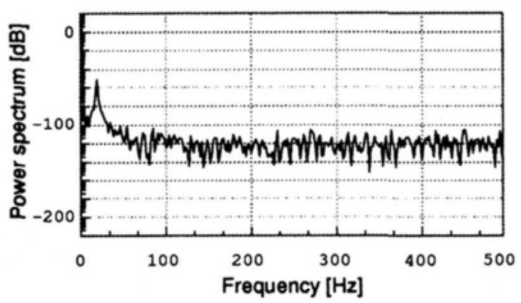

(b) Power spectrum - Experimental results.

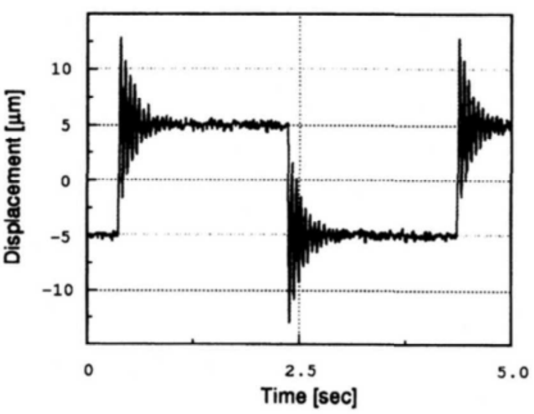

(c) Step response - Theoretical results.

Fig. 6. Results of the system without a controller.

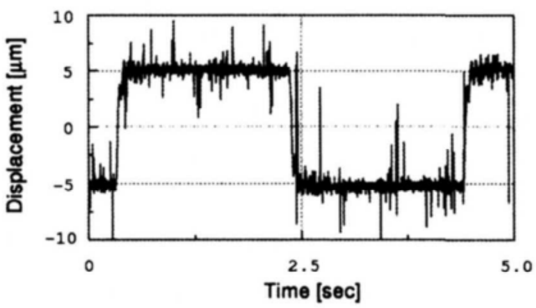

(a) Step response - Experimental results.

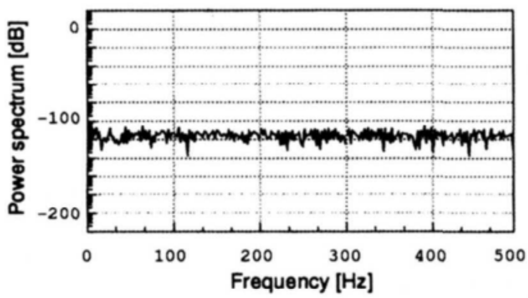

(b) Power spectrum - Experimental results.

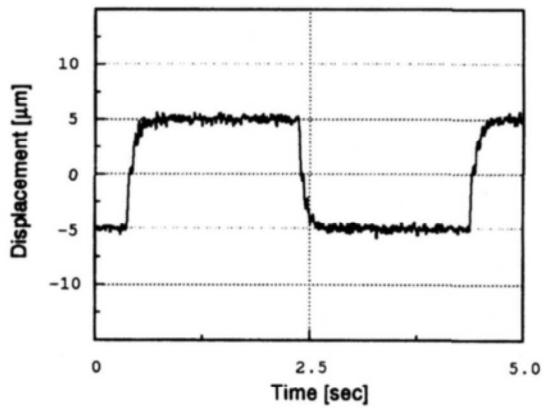

(c) Step response - Theoretical results.

Fig. 7. Results of the system with an LQG controller.

6. Conclusion

We proposed an LQG controller design method for a flexible microactuator with sensor noise. Optimal observer gains can be computed by adopting a stochastic approach to the problem, leading to the Kalman filter. Experimental and numerical results verified that the proposed design method is effective for flexible microactuator control applications.

Acknowledgment

The authors would like to thank Dr. Fumio Fujisawa and Mr. Raphael London Mwangobola who made many valuable suggestions for the paper.

References:

1) J. Curie, P. Curie and C.R. Acad, Sci. Paris, **91**, 294 (1880).
2) Pl Langevin, Brev. Franc., **505**, 703 (1918).
3) H. Kawai, "The Piezoelectricity of Poly (vinylidene Fluoride)", Jpn. J. Appl. Phys., **8**, 975-976 (1968).
4) N. Murayama, N. Nakamura, H. Obara, and M. Segawa, "The Strong Piezoelectric in Poly Vinylidene fluoride (PVDF)", Ultrasonics, **14**, 15-23 (1967).
5) G.M. Sessler, "Piezoelectricity in Polyvinylidene Fluoride", J. Acoust. Soc. Am., **70**, 1596-1608 (1981).
6) W. Sachse and N. Hsu, "Ultrasonic Transducers", in Encyclopedia of Materials Science and Engineering, edited by M.B. Bever, Pergamon, New York, 5192-5198 (1988).
7) "KYNAR Piezo Film Technical Manual", Pennwalt Corp., 48-52 (1987).
8) M. Sasaki, H. Inooka, "Dynamic characteristic and Control of a High-Polymer Piezoelectric Actuator", Trans. JSME, **57**-534, 174-178 (1991).
9) M. Sasaki, P.K.C. Wang, "Piezopolymer Flexible Micro-Manipulator", Proc. KACC'95, 2-2, 1459-1464 (1991).
10) M. Sasaki, "Piezopolymer Bimorph Flexible Micro-Actuator", Proc. MOVIC, 368-373 (1992).
11) M. Okugawa, M. Sasaki, K. Suzuki, M. Ishihara, "Optimal Force Tracking Control of a Piezoelectric High-polymer Actuator", Proc. 5th ICAS, Sendai, Japan, 602-611 (1994).
12) M. Okugawa, M. Sasaki, "Control of a Flexible Micro-Manipulator", Proc. JSME ROBOMEC'95, Kawasaki, Japan, **95**-17 (A211), 133-136 (1995) (in Japanese).
13) M. Okugawa, M. Sasaki, "Controller Design Method of a Flexible Micro-Manipulator", Proc. MIMR'95, Sendai, Japan, 71-74 (1995).
14) R.E. Kalman, "A New Approach to liner Filtering and Prediction Problem", Trans. ASME, Series, D, Journal of Basic Engineering, **82**, 35-45 (1960).
15) T. Takeda, T. Kitamori, "A Design Method of Linear Multi-Input-Output Optimal Tracking Systems", Transactions of Society of Instrument and Control Engineers, **14**-4, 359-364 (1978) (in Japanese).
16) A. Grace, A.J. Laub, J.N. Little, and C.M. Thompson, "MATLAB Control System Toolbox Ver.3.03 User's Guide", The Math Works Inc. (1992).

Name:
Minoru Sasaki

Affiliation:
Associate Professor, Department of Mechanical Engineering, Faculty of Engineering, Gifu University

Address:
1-1, Yanagido, Gifu, 501-11, Japan

Brief Biographical History:

1985 - Joined Department of Mechanical Engineering, Tohoku University as a research associate
1991 - Visiting Professor, University of California, Los Angeles
1993 - Appointed associate professor of Department of Mechanical Engineering Gifu University

Main Works:

- "Piezopolymer Flexible Micro-Actuator with Multi-Degrees of Freedom", fifth International Conference on Adaptive Structures", 513-522, Edited by J. Tani. et al., Technomic Publishing Co., Inc., Lancaster, 1995.

Membership in Learned Societies:

- The Institute of Electrical and Electronics Engineers (IEEE)
- The Japan Society of Mechanical Engineers (JSME)
- The Robotics Society of Japan (RSJ)
- The Society of Instrument and Control Engineers (SICE)
- The Japan Society for Aeronautical and Space Sciences

Name:
Masayuki Okugawa

Affiliation:
Graduate Student, Department of Mechanical Engineering, Faculty of Engineering, Gifu University

Address:
1-1 Yanagido, Gifu, 501-11 Japan

Brief Biographical History:

1994 - Received the B.E. degree in Mechanical Engineering from Gifu University

Main Works:

- "Optimal Force Tracking Control of a Piezoelectric High Polymer Actuator", Fifth International Conference on Adaptive Structures, 602-611, Edited by J. Tan et al., Technomic Publishing Co., Inc., Lancaster, 1995.

Membership in Learned Societies:

- The Japan Society of Mechanical Engineers
- The Institute of Systems, Control and Information Engineers